Advances in Machinery, Materials Science and Engineering Application IX
M. Chen et al. (Eds.)

doi:10.3233/ATDE230472

Effect of Installation Errors of Helical Gear on Bearing Capacity

Heng LUAN [a], Xiantao SHU [b] and Jiabing WANG [b,1]
[a] *Senior Engineer (Mechanical and Electrical) and Master of Management Studies, Qingdao Human Resources Development Research and Promotion Center, 15 Shandong Road, Shinan District, Qingdao, China.*
[b] *Department of Mechanical Engineering, School of Mechanical Automation, Wuhan University of Science and Technology, 947 Heping Avenue, Qingshan District, Wuhan, China*

Abstract. Broken tooth roots due to mounting errors in helical gears at high speeds and heavy loads are a common problem in steel mills. Based on the contact characteristics of helical gears, this paper uses the finite element method to simulate the bending stress at the root of the pinion gear and the contact stress at the tooth surface under two cases of different center distance error and axis parallelism error, analysis of the reasonable fluctuation range of the maximum principal stress and the maximum contact stress is obtained by fitting the relationship between these two stresses and the variation of the two errors, and then the bending and contact strengths are calibrated based on the simulation results. The study shows that the gears' strength can meet the requirements when installed according to the grade seven gear transmission accuracy of the national standard of involute cylindrical gear accuracy, under the case of center distance error; under the case of the parallelism error, the inclination angle should be controlled within 0°3 '2" to meet the minimum service safety factor conditions. The steel mills strictly control the above-mentioned installation accuracy when using helical gear drives, which can avoid gear tooth root breakage and improve the efficiency and reliability of gear drives.

Keywords. Helical gear, gear mounting error, finite element method, bending stress, contact strength.

1. Introduction

The helical gear drive (first stage reduction) in the main gearbox is an important part of the steel mill in high-speed and heavy-duty tasks. Based on the data, the helical gear drive process is often affected by the stress concentration condition at the gear contact [1-2], and when the threshold value is exceeded, the tooth root breaks (as shown in figure 1) [3].

Once the main gearbox pinion is marked by ink, the relationship between the loading contact point of the helical gear (as shown in figure 2) and the position of the corresponding point reflects the existence of mounting errors in the helical gear, which

[1] Jiabing WANG, Corresponding author, Department of Mechanical Engineering, School of Mechanical Automation, Wuhan University of Science and Technology, 947 Heping Avenue, Qingshan District, Wuhan, China; E-mail: wang128ve980@163.com.

will determine the load carrying capacity and fatigue life of the gear under standard machining errors [4]. To reduce the tooth root bending stress and tooth contact stress of the gear, adjustments are made mainly from two aspects of the gear mounting error: parallelism error and center distance error [5-6].

The contact characteristics of helical gears under dynamic loading are tedious and distorted using traditional empirical equations to solve. A mathematical model for quantitative evaluation of assembly errors based on key components is used to parametrically analyze the effect of assembly on contact performance [7-8]. The tooth structure, force parts and external conditions [9] are incorporated into the analysis to fully adapt to the work of the gear reducer. The dynamic visualization of the helical gear loading situation by FEA [10], and the analysis efficiency of the contact surface stress situation is improved by mesh pre-processing [11]. Locate the most concentrated gear stress [12-13] by simulating the change in gear contact force. Based on the ideal equation calibration of the helical gear train [14], the analysis results are used to adjust the reasonable range of the helical gear assembly error.

The three-dimensional model of the gear pair of the main gearbox is established herein, and the changes of the pinion tooth root bending stress and tooth surface contact stress under different center distance error and axis parallelism error of the helical gear are analyzed by the finite element method, and the finite element analysis results are calibrated by combining the tooth root bending strength calibration formula and tooth surface contact strength calibration formula, and the suitable installation error range is determined.

Figure 1. Fracture diagram of teeth root.

Figure 2. Gear sub contact spot diagram.

2. Basic Parameters of Gears

Based on the steel mill reducer drawing, the large gear is made of 42CrMo with Poisson's ratio of 0.28, modulus of elasticity E of 2.06×10^5Mpa, tooth surface carburized and quenched, and hardness range of HRC54-60. The pinion is made of 17Cr2Ni2Mo with Poisson's ratio of 0.3, modulus of elasticity E of 2.1×10^5MPa, tooth surface carburized and quenched, and hardness range of HRC56-61. The large gear has 110 teeth with a correction factor of 0. Other parameters resemble those of the gear shaft. The basic parameters of the gear shaft are shown in table 1.

Table 1. Basic parameters of gear shaft.

Name	Initial value	Description	Name	Initial value	Description
MN	28	Normal module	HA	--	Tooth addendum

Z	23	Tooth number	HF	--	Tooth dedendum
ALPHA	20	Pressure angle	X1	0.337	Pinion modification coefficient
BETA	10	Spiral Angle	D	--	Reference diameter
B	680	Tooth width	DB	--	Base circle diameter
HAX	1.0	Tooth Addendum coefficient	DA	--	Tip diameter
CX	0.25	Headspace coefficient	DF	--	Root diameter

3. Model Building

3.1. Three-dimensional Model Building

Based on the original dimensions of the main gearbox, the 3D solid model of the helical gear was accurately created by parametric modeling using Creo 2.0. The tooth faces in the modeling process were involute, and the scan path of the tooth profile was an indexed cylindrical helix.

3.2. Contact Surface Setting and Meshing

The three tooth surfaces that may be in contact with the gear shaft were selected to define the contact surface. The Type was set to Friction type and the friction coefficient was set to 0.1.

The tetrahedral meshing method was used for the complex structure of the gear shaft. The large gear has a simple structure, and the sweep method [15] was used to automatically generate a hexahedral mesh. To control the different minimum cell sizes, the active wheel gear shaft and driven wheel large gears were divided into separate meshes with multi-zone mesh size control. Additionally, the mesh refinement was performed for the contact tooth surface, and the gear shaft size was set to 150 mm, the large gear size was set to 250 mm, and the mesh size of the contact area was 5 mm.

3.3. Constraint and Loading

The gear system operated with a limited number of degrees of freedom, including circumferential and radial displacements, as well as displacement and axial overturning of both faces. In ANSYS, a remote displacement condition was used to constrain the pinion gear, allowing only one degree of freedom of rotation about the Z-axis. In contrast, a fully constrained condition with fixed support was used for the large gear [16]. The counter clockwise torque, calculated using the rated power of the motor, is applied to the pinion input by the following equation:

$$T = \frac{9.55\times10^6 P}{N} \tag{1}$$

Where P is the rated power of the motor at 8000kW and N is the rated speed of the motor at 180r/min. The applied torque is calculated to be 424.44kN·m. The applied constraint and load are given in figure 3.

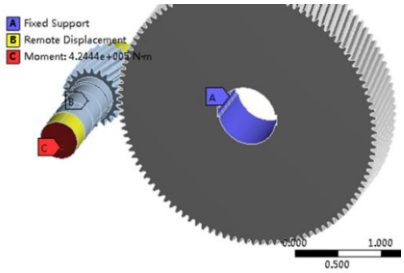

Figure 3. The applied constraint and load.

3.4. Constraint and Loading

Based on the gear meshing characteristics and field conditions, the gear shaft is used as the object of study in this paper. The first principal stress, the third principal stress and the contact stress of the gear shaft were solved by the solver. The solved results are shown in figure 4.

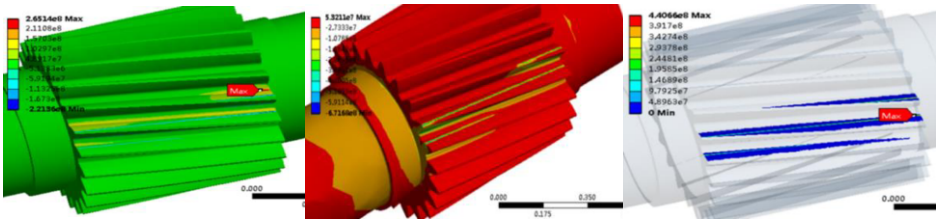

(a) First principal stress. (b) Third principal stress. (c) Contact stress.

Figure 4. The Gear shaft stress nephogram.

Figure 4 displays the maximum principal stress at the gear teeth root alongside the maximum contact stress near the contact position. Specifically, the root of the tooth experiences a first principal stress of 265.11 MPa and a third principal stress of 53.211 MPa, indicative of a three-way tensile stress state as per material mechanics theory. Consequently, the bending strength of the tooth root should be calibrated based on the first principal stress. Additionally, the tooth surface encounters a maximum contact stress of 440.66 Mpa.

4. Analysis of Simulation Result

4.1. Finite Element Simulation Analysis of Helical Gears with different Center Distance Errors

The helical gear model was used to assemble gear pairs with a center distance error of 0.04 mm. To ensure the comparability of the maximum principal stress and tooth contact stress under different errors, the control variable method was used to ensure the consistency of the gear meshing points during the whole assembly process. After preprocessing, the solver analyzes the first principal stress and contact stress within the

gear shaft with errors ranging from -0.08 mm, -0.04 mm, -0 mm, 0.04 mm, 0.08 mm, and 0.12 mm. Figure 5 shows the cloud plots of the first principal stress and contact stress distribution for -0.08 mm. The maximum first principal stress and the maximum contact stress are shown in figure 6 and are listed in table 2.

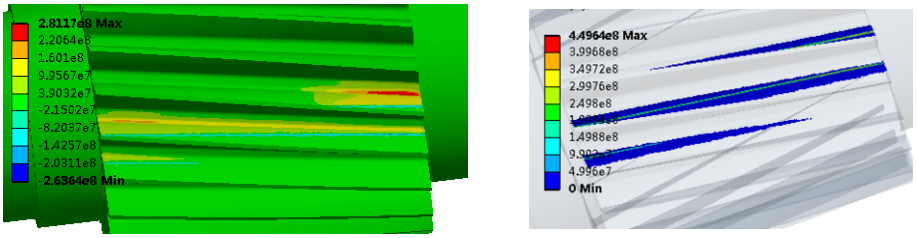

(a) First principal stress: 281.17MPa. (b) Contact stress: 449.64MPa.

Figure 5. The center distance error is -0.08mm.

Table 2. Corresponding gear shaft main stress and contact stress under center distance error.

Center distance error value/ mm	Maximum bending stress at root/ MPa	Maximum contact stress of tooth surface/ MPa
-0.08	281.17	449.64
-0.04	267.01	443.24
0.00	265.14	440.16
0.04	266.71	446.80
0.08	280.69	452.47
0.12	317.72	471.81

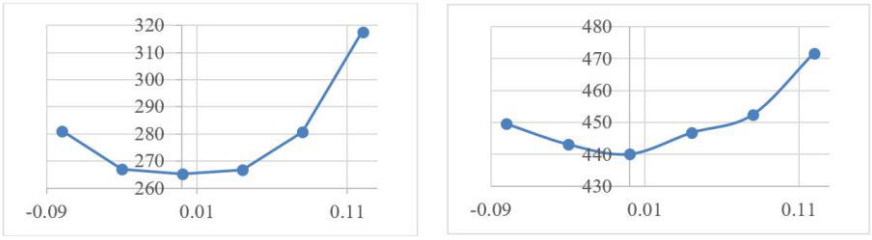

(a) Curve of maximum bending stress of tooth root and deviation of center distance.

(b) Tooth surface maximum contact stress and center distance deviation curve.

Figure 6. The maximum stress of gear shaft tooth under different center distance error.

Figure 6 illustrates that the maximum tooth root stress and the maximum contact stress on the gear shaft tooth surface are positively correlated with the center distance error. The rate of increase increases slowly at first, but eventually rises sharply.

4.2. Fatigue Strength Calibration of Gears with Center Distance Error

1) Gear bending strength safety factor calculation formula:

$$S_F = \frac{\sigma ST_{NT\delta rel_{Rrel_{XFlim}}}}{\sigma_{FAnsys}} \tag{2}$$

Where, based on the reference [17-18], $\sigma_{FAnsys}$is the bending stress calculated by finite element of gear shaft; σ_{Flim}=324MPa, the bending ultimate fatigue stress of gear; Y_{ST}=2.0, the stress correction factor of test gear; Y_{NT}=1.1, the life factor calculated by bending strength; $Y_{\delta rel}$=0.95, the relative tooth root fillet sensitivity factor; Y_{Rrel}=0.99, the relative tooth root surface condition factor; Y_X =0.75, the dimension factor calculated by bending strength.

2) Calculation formula of safety factor of gear contact strength:

$$S_H = \frac{\sigma NT_{LVR_{WX_{Hlim}}}}{\sigma_{HAnsys}} \tag{3}$$

Where, based on the reference [19-20], σ_{Hlim}=1500MPa, the the contact stress calculated by finite element of gear. $\sigma_{HAnsys}$is the gear contact fatigue limit stress; Z_{NT}=1.0, the contact strength calculation life factor; Z_{LVR}=0.85, the lubricant film influence factor; Z_W=1.0, the working hardening coefficient of tooth surface; Z_X=0.75, the contact strength calculation size.

When the use of gears requires general reliability, the minimum safety factor is taken as S_{Hmin}=1.0 and S_{Fmin}=1.25. By substituting the finite element simulation results in table 2 into equations (2) and (3) respectively, the root bending strength safety factor and tooth contact strength safety factor can be obtained for different center distance errors, as shown in table 3.

Table 3. Coefficient of safety for root bending strength and tooth surface contact strength at different center distances.

Center distance error value/ mm	Tooth root bending strength safety factor SF	Tooth surface contact strength safety factor SH
-0.08	1.79	2.13
-0.04	1.88	2.16
0.00	1.90	2.17
0.04	1.89	2.14
0.08	1.79	2.11
0.12	1.58	2.03

GB10095-88 stipulates that the limit deviation of the accuracy of the seven-stage gear drive with center distance between 1600mm and 2500mm is ±0.115mm, and the limit deviation of the accuracy of the six-stage gear drive is ±0.08mm. As highlighted in table 3, the deviation of the center distance between -0.08mm and 0.12mm can keep the tooth root bending strength and tooth surface contact strength The safety factor

meets the requirements of use, and the gear strength requirements are fully met when the six-stage transmission accuracy is used for installation on site.

4.3. Simulation Analysis of Helical Gears with Parallelism Error

The gear pair assembly with parallelism error of 0.1mm interval was established. The stresses in the gear shaft were analyzed in the error range of 0 mm to 1.2 mm, and the clouds of the first principal stress and contact stress distribution at a parallelism error of 0.2 mm are shown in figure 7. The maximum first principal stresses and maximum contact stresses are shown in table 4 and figure 8.

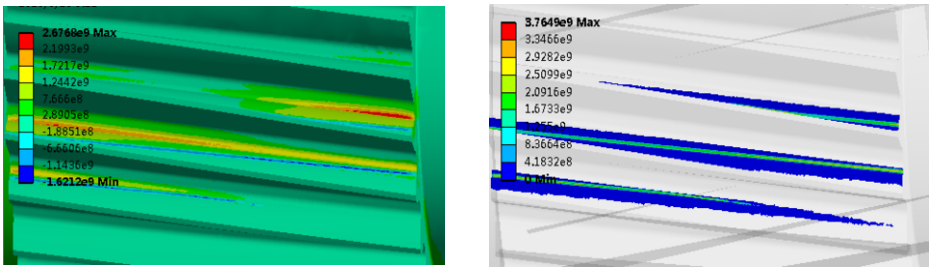

(a) First principal stress: 267.68MPa. (b) Contact stress: 376.49MPa.

Figure 7. Parallelism error of 0.2mm.

Table 4. Bending and contact stresses in gears with different parallelism errors.

Shaft end offset/ mm	Corresponding dip Angle	Maximum principal stress/ MPa	Maximum contact stress/ MPa
0.0	0°0'0"	250.38	352.98
0.2	0°1'1"	267.68	376.49
0.4	0°2'1"	291.00	433.59
0.6	0°3'2"	362.35	499.09
0.8	0°4'3"	472.94	683.74
1.0	0°5'2"	559.11	888.31
1.2	0°6'4"	690.24	1303.60

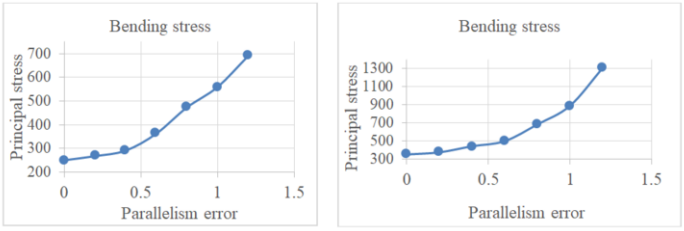

(a) Maximum bending stress at the root of the tooth versus parallelism error. (b) Maximum contact stress on tooth face versus parallelism error.

Figure 8. Maximum stresses in gear shaft teeth with different parallelism errors.

As seen from the scatter plot of the gear shaft stress distribution, the tooth root bending stress and tooth surface contact stress show a nonlinear increase with the increase of the shaft end offset, i.e., the increase of the gear mounting unevenness. At the offset angle of 0°0'0" to 0°2'1", the changes of both bending stress and contact

stress are small, with bending stress fluctuating within 50 MPa and contact stress fluctuating within 100 MPa. However, deflection distances exceeding 0°2'1" lead to a rapid increase in bending and contact stresses.

4.4. Fatigue Strength Calibration of Gears with Parallelism Errors

Similar to the calculations in the previous section, the magnitude of the bending strength and contact strength safety factors for gears with different parallelism errors were obtained, as shown in table 5.

Table 5. Bending strength and contact strength safety factors of gears with different parallelism errors.

Shaft end offset/ mm	Corresponding dip Angle	Tooth root bending strength safety factor SF	Tooth surface contact strength safety factor SH
0.0	0°0’0”	2.008	2.709
0.2	0°1’1”	1.878	2.540
0.4	0°2’1”	1.728	2.205
0.6	0°3’2”	1.388	1.916
0.8	0°4’3”	1.063	1.399
1.0	0°5’2”	0.899	1.076
1.2	0°6’4”	0.728	0.734

Analysis of table 5 reveals that gear root bending strength safety factor and tooth contact strength safety factor fall below standards for general gear use when gear shaft end inclination exceeds 0°4'3", rendering the gears unfit for safe operation. To meet minimum use safety factor standards, a gear shaft end inclination not exceeding 0°3'2" is necessary, with additional considerations taken for dynamic loading and other potential factors.

5. Conclusion

The paper conducts finite element analysis on the center distance error and parallelism error of the gear installation while performing strength checks on the corresponding finite element analysis results of tooth root bending strength and tooth face contact strength. The results show that:

(1) In the case of centre distance error, according to the national standard of involute cylindrical gear accuracy, the strength of the gear has fulfilled the requirements when installed in accordance with class 7 gear transmission accuracy, while the site is generally installed in accordance with class 6 gear transmission accuracy, so the strength of the gear fully meets the requirements.

(2) In the case of parallelism error, according to the actual adjustable eccentricity of the shaft end on site, the inclination of the gear shaft end should be controlled within 0°3'2" under the condition of meeting the minimum safety factor for operation.

In summary, the steel mill has attained favorable outcomes in regularly measuring and adjusting the two gear shaft flatness errors of the reducer.

References

[1] Wang NN. Fracture reason analysis for helical gear shaft of reducer. Coal Mine Machinery. 2013.

[2] Guan L and Wang N N. fracture reason analysis for helical gear shaft of converter tilting mechanism senior reducer. Advanced Materials Research. 2012: 605-607, 824-827.
[3] Feng L and Dewen K. Fault diagnosis of tooth root crack in helical gear. 2016 13th International Conference on Ubiquitous Robots and Ambient Intelligence (URAI). 2016; pp. 686-691.
[4] Li W, Zhai P, Tian J and Luo B. Thermal analysis of helical gear transmission system considering machining and installation error. International Journal of Mechanical Sciences. 2018.
[5] Lin T and He Z. Analytical method for coupled transmission error of helical gear system with machining errors, assembly errors and tooth modifications. Mechanical Systems and Signal Processing. 2017; 91: 167-182.
[6] Hanhan S, Yunbo S, Wei W L and Yang Z. Sensitivity analysis of face gear installation error. Proceedings of the 2019 International Conference on Precision Machining, Non-Traditional Machining and Intelligent Manufacturing (PNTIM 2019), 2019.
[7] Zhang M, Zhang Z and Shi L. A new assembly error modeling and calculating method of complex multi-stage gear transmission system for a large space manipulator. Mechanism and Machine Theory. 2020; 153: 103982.
[8] Huang KJ and Su HW. Approaches to parametric element constructions and dynamic analyses of spur/helical gears including modifications and undercutting. Finite Elem. Anal. Des. 2010; 46: 1106-1113.
[9] Liang Y, Caballero JM, Juanatas R, Wei Y, Bao Z and Jin W. Design and finite element analysis of the three rings gear reducer. World Automation Congress (WAC), San Antonio, TX, USA, 2022; pp. 252-256
[10] Boonmag V, Phukaoluan A, Wisesook O and Pluphrach G. Comparison of bending stress and contact stress of helical gear transmission using finite element method. International Journal of Mechanical Engineering and Robotics Research. 2018.
[11] Hedrih KS and Nikolić-Stanojević V. A model of gear transmission: Fractional order system dynamics. Mathematical Problems in Engineering. 2010.
[12] Huang ZH, Zhang XJ and Zhou YJ. Simulation of contact force of involute gear meshing. Journal of Central South University (Science and Technology). 2011; 42(2): 379-383.
[13] Kumar SP, Suman KN, Nagaraju BV and Ramanjaneyulu S. Contact stress analysis of structural steel gears under misalignment of shafts. Lecture Notes on Multidisciplinary Industrial Engineering. 2019.
[14] Hedrih KS and Nikolić-Stanojević V. A model of gear transmission: fractional order system dynamics. Mathematical Problems in Engineering. 2010.
[15] Roca X, Sarrate J and Huerta A. A new least-squares approximation of affine mappings for sweep algorithms. Engineering with Computers. 2010; 26: 327–337.
[16] Yang JT and Zhang K. Finite element analysis of gears of reducer based on ANSYS. Journal of Wuhan University of Science and Technology. 2014; 37(4):288-291.
[17] Li WL. Study on the dynamic characteristics of helical gear transmission with tooth friction. Harbin Institute of Technology. 2013.
[18] Sun JG, Lin TJ, Li RF and Liu W. Finite element analysis of involute gear dynamic contact and the effect of shape modification. Mechanical Transmission. 2008; (02):57-59+1.
[19] Tang JY, Peng FJ and Huang YF. Numerical analysis of the dynamic stress variation law of gears under impact loading. Vibration and Impact. 2009; 28(8):138-143.
[20] Sun T and Hu H. Nonlinear dynamics of a planetary gear system with multiple clearances. Mechanism and Machine Theory. 2003; 38(12): 1371-1390.